

Mississippi State University

Scholars Junction

Theses and Dissertations

Theses and Dissertations

1-1-2017

Development of a Portable Laser-Induced Fluorescence Sensor

Adam Oswalt Powers

Follow this and additional works at: <https://scholarsjunction.msstate.edu/td>

Recommended Citation

Powers, Adam Oswalt, "Development of a Portable Laser-Induced Fluorescence Sensor" (2017). *Theses and Dissertations*. 1426.

<https://scholarsjunction.msstate.edu/td/1426>

This Graduate Thesis - Open Access is brought to you for free and open access by the Theses and Dissertations at Scholars Junction. It has been accepted for inclusion in Theses and Dissertations by an authorized administrator of Scholars Junction. For more information, please contact scholcomm@msstate.libanswers.com.

Development of a portable laser-induced fluorescence sensor

By

Adam Powers

A Thesis
Submitted to the Faculty of
Mississippi State University
in Partial Fulfillment of the Requirements
for the Degree of Master of Science
in Physics
in the Department of Physics and Astronomy

Mississippi State, Mississippi

August 2017

Copyright by

Adam Powers

2017

Development of a portable laser-induced fluorescence sensor

By

Adam Powers

Approved:

Ariunbold Gombojav
(Major Professor)

Hendrik F. Arnoldus
(Committee Member/Graduate Coordinator)

Donna M. Pierce
(Committee Member)

Rick Travis
Dean
College of Arts and Sciences

Name: Adam Powers

Date of Degree: August 11, 2017

Institution: Mississippi State University

Major Field: Physics

Major Professor: Ariunbold Gombojav

Title of Study: Development of a portable laser-induced fluorescence sensor

Pages in Study: 32

Candidate for Degree of Master of Science

This thesis describes the design and construction of a portable laser induced fluorescence sensor. The objective was to create a low-cost, versatile, and modular laser induced fluorescence sensor for agricultural remote sensing. The sensor module should be able to be integrated with different pieces of hardware. The objective was successfully accomplished with the creation of a sensor module that met all of the requirements. The sensor module integrates with a handheld unit for reading and visualizing the data that was constructed and is described in this work. Performance testing and experiments were carried out with the sensor module in the handheld device with a focus on plant physiology. In particular, chlorophyll fluorescence related to stress and ripeness was studied and fungal toxins found in corn were detected with this device. Ongoing work consisting of mounting the sensor module to an unmanned aerial vehicle and testing in flight is described.

DEDICATION

*To my wife, **Katherine,***

For loving and supporting me through my education and life

*To my parents, **Blair and Irene Powers,***

For raising me with love and giving me inspiration and motivation through my academic
career.

ACKNOWLEDGEMENTS

I would like to thank the Department of Physics and Astronomy and everyone involved for their exemplary performance as teachers, mentors, and friends. I would like to especially acknowledge Dr. Ariunbold Gombojav for accepting me as his student and allowing me to research under him. Dr. Henk Arnoldus and Dr. Donna Pierce deserve the highest praise for being among the best teachers I've ever had. I am honored they accepted to serve on my committee.

To my colleagues and fellow researchers: Shane Clark, Supriya Nagpal, Prakash Adhikari, and Nava Subedi, I give my utmost gratitude for all their help through my graduate studies, both for the comradery in our classes together and assistance in research.

TABLE OF CONTENTS

DEDICATION	ii
ACKNOWLEDGEMENTS	iii
LIST OF TABLES	vi
LIST OF FIGURES	vii
CHAPTER	
I. INTRODUCTION	1
1.1 Motivation	1
1.2 Objective.....	1
II. BACKGROUND	3
2.1 Laser-induced Fluorescence	3
III. LIF SENSOR MODULE CONSTRUCTION	6
3.1 Hardware	6
3.1.1 Optics and Spectrometer.....	6
3.1.2 Controlling Electronics.....	9
3.2 Software.....	11
3.2.1 Spectrometer Control.....	12
3.2.2 Graphical User Interface (GUI).....	13
IV. DATA COLLECTION AND ANALYSIS	15
4.1 Calibration and Performance Testing.....	15
4.2 Chlorophyll Fluorescence of Vegetation.....	16
4.3 Inspection of Fruit Ripeness.....	20
4.4 Aflatoxin Detection	22
V. CONCLUSION AND FUTURE WORK.....	25
5.1 Ongoing Work	25
5.2 Conclusion.....	27

5.3	Future Work.....	27
REFERENCES	29
APPENDIX		
A.	MATERIALS	31
A.1	Cost Breakdown	32

LIST OF TABLES

A.1	An itemized listing with costs for all parts used.....	32
-----	--	----

LIST OF FIGURES

2.1	Jablonski diagram of fluorescence process.	4
3.1	Diagram of optics system comprising the sensor module	8
3.2	Hamamatsu C12666MA micro spectrometer, shown with pen for scale	8
3.3	The sensor module by itself.....	10
3.4	The sensor module integrated with the handheld unit.....	11
3.5	Control diagram of the sensor module in the handheld unit	13
3.6	Example of GUI	14
4.1	Spectrum taken of a helium lamp along with known spectral lines.....	16
4.2	Spectra of Spruce at 405nm excitation [1].	17
4.3	Chlorophyll fluorescence spectra of unstressed (left) and stressed (right) water oak leaves.	19
4.4	Image of two water oak leaf samples, an unstressed (left) and a stressed (right) leaf.	20
4.5	Chlorophyll fluorescence of a Banana with the F690/F740 ratio plotted against days.	21
4.6	Chlorophyll fluorescence of a Granny smith apple with the F690/F740 ratio plotted against days.	22
4.7	Fluorescence spectra collected from kernels with and without aflatoxin present	23
5.1	A Control diagram for the sensor module and UAV electronics	26

CHAPTER I

INTRODUCTION

1.1 Motivation

Fluorescence has been used as a powerful tool for many decades to explore and evaluate many properties not available to direct observation of reflected light. Its use ranges from medical diagnostics [2], historical monument preservation efforts [1], and water characteristics, including potability or identification of organic matter [1, 3]. A large amount of effort in fluorescence spectroscopy is focused towards agricultural and plant physiological monitoring. Quantifications of soil content [4], presence of invasive species and disease [11], and diagnostics of plant stress [5] have all been performed. Many of these applications have been performed either in a laboratory setting or in the field with large and/or expensive equipment. With the ever increasing manufacturing capabilities and subsequent decrease in cost of equipment, the power of fluorescence spectroscopy as a high throughput tool for everyone can be realized.

1.2 Objective

Portable laser-induced fluorescence systems can cost thousands of dollars and are quite frequently only designed for measurements of certain types of fluorescence [3]. Usually these include photomultiplier tubes (PMT) and filters as their selectors, limiting their use outside of the intended target. The goal of this system was to create a versatile fluorescence system that avoids the shortcomings of these systems. There were several

design goals in mind for this system, including cost-effectiveness, modularity, and simplicity, both in construction and in use. The modularity of the system will allow a base sensor module to connect with different pieces of hardware, such as the handheld device described here, an unmanned aerial vehicle (UAV), computers, or other devices. With advancements in manufacturing techniques of spectrometers, such as nanoimprinting technologies, more compact and less expensive spectrometers are able to be fabricated. The use of a 'micro-spectrometer' manufactured using these techniques instead of filters and PMTs allows for not only fluorescence measurements, but also reflectance readings. It also has the ability to easily observe many types of fluorescence without having to physically change any hardware of the device. With the ability to quickly switch out excitation sources, more fluorescence targets can be explored. Detailed in this paper is also a handheld device for integrating with the sensor module. This allows anyone already familiar with fluorescence spectroscopy to pick up the device and begin using it on their farm, garden, or household.

This thesis is organized as follows. A brief background on laser induced fluorescence will precede chapters detailing the design and construction of the sensor module and handheld unit. Several tests that were performed with the device will then be shown, followed by other ongoing research using the sensor module.

CHAPTER II

BACKGROUND

2.1 Laser-induced Fluorescence

When UV or visible wavelength photons are incident on certain organic molecules, they can either be scattered elastically or absorbed. If the photon energy falls within the absorption range of the molecule, it is absorbed. This energy can promote an electron to a higher electronic energy state, where it subsequently relaxes without radiation to its lowest excited state. Then, after a very brief time period on the order of nanoseconds, they decay, emitting photons of a longer wavelength than the original absorbed light [1]. When this occurs, it is known as fluorescence. A simple diagram, known as a Jablonski diagram, showing this process is provided in Figure 2.1.

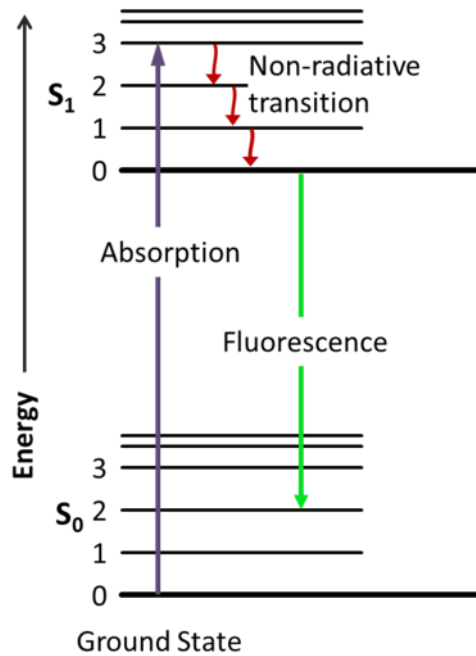


Figure 2.1 Jablonski diagram of fluorescence process.

When the excitation source is a laser, this process is referred to as laser-induced fluorescence (LIF). Due to the initial non-radiative decay after absorption, the fluorescence is independent of the absorbed photon energy provided only that the absorbed energy falls within its absorption range. By using different excitation wavelengths and measuring the fluorescence spectra, information on molecules in the system being studied can be found [1]. A typical remote sensing LIF fluorescence system is as follows. A laser excitation source is incident on the target and light from the target is collected via a telescope. Once gathered, long pass filters are used to remove the reflected light of the laser. The unfiltered light is directed to a spectrometer, which measures the wavelengths of light comprising this signal. A common strategy for removing ambient

and background light from the spectra is to modulate the laser and synchronize this modulation to the gate of the spectrometer. To reduce noise in the signal, measurements of the same target can be taken and averaged [1].

CHAPTER III

LIF SENSOR MODULE CONSTRUCTION

3.1 Hardware

Many LIF systems become cost-prohibitive for widespread use due to expensive electronics, spectrometers, and lasers for excitation. However, with the ever decreasing cost of electronics and solid state devices, it is becoming easier than ever to make things more cost effective. All casing and mounting fabricated for this work was done using 3D printing. A complete breakdown of cost for the device can be found in Appendix A.1. In this section, the physical design of the sensor module is introduced, beginning with a description of the optical system, followed by the electronics that control the system.

3.1.1 Optics and Spectrometer

At the heart of this LIF device is the C12666MA Micro spectrometer from Hamamatsu Photonics, shown in Figure 3.2. Small in both cost and size, it is easy to integrate into a portable system. The ability to manufacture such a small spectrometer comes from nanoimprinting a reflective, concave, blazed grating to disperse the incident light into its component wavelengths, and a micro sized, etched CMOS sensor for intensity detection of these photons. This micro spectrometer has a spectral response in the visible wavelengths ranging from 340 nm to 780 nm through 256 bins with 15 nm maximum spectral resolution. After several configurations and rounds of lab testing, the simplest optics system was chosen for light collection and focusing onto the

spectrometer's slit. This involves a single plano-convex, NBK-7 50.8 mm lens with a 60 mm focal point from Thorlabs, Inc. An inexpensive colored glass long pass filter corresponding to the wavelength of the excitation source was used to eliminate elastic back scattering of the incident light. The main excitation source used in the device is a 405 nm diode laser with integrated and variable focusing optics. The power of this inexpensive diode laser is adjustable from 0 – 150 mW. The long pass filter used with this source has a cutoff wavelength of 420 nm. The laser in the final arrangement is positioned adjacent to the optics. Though simple, this introduces a distance dependence on the measurements. To counter this distance dependence, the laser can be easily steered via the mounting system, allowing quick and easy distance tuning. This simple setup is shown in Figure 3.1. This optics systems and arrangement of source was chosen for its low number of components, cost, simplicity, and versatility. This system allows for the laser source and corresponding filter to be quickly and easily exchanged for another.

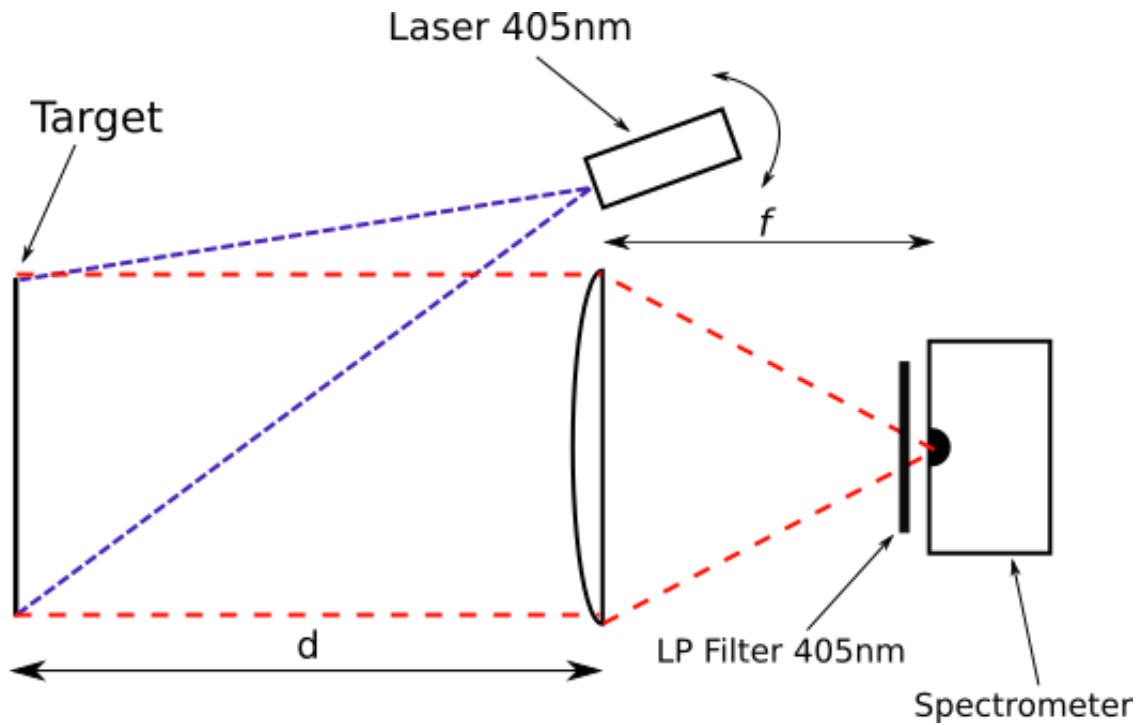


Figure 3.1 Diagram of optics system comprising the sensor module

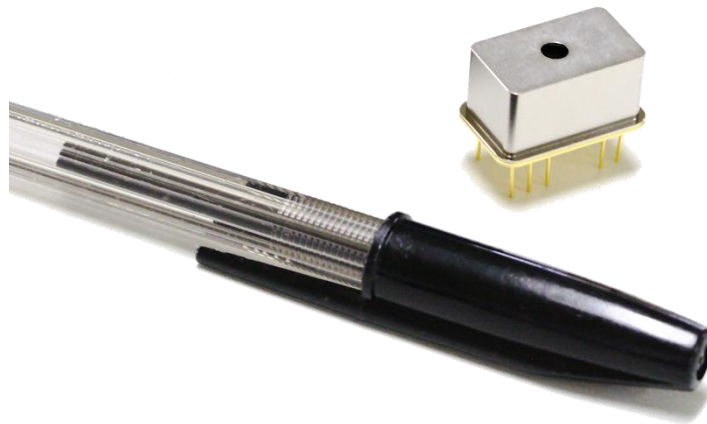


Figure 3.2 Hamamatsu C12666MA micro spectrometer, shown with pen for scale

3.1.2 Controlling Electronics

Because of its compactness, the Hamamatsu spectrometer requires extra electronics to interface with it. In addition to controlling collection parameters like integration time and gain, the light collection itself must be triggered. In order for the information gathered by the spectrometer to be useful, it must be able to be stored, referenced, or visualized. To achieve this, two distinct pieces of electronic hardware were used. At the most basic level of spectrometer interfacing, a microcontroller, the Arduino Nano, was used. This communicates directly with the spectrometer for collection, parameter control, and data storage on an SD card. For higher level communication and data storage, visualization, and analysis, a Raspberry Pi 3 Model B (RPI) was used running the Linux based Raspbian operating system. The advantage of using the RPI in the system is, because it features a full operating system, one has the ability to choose which programming language and software tools are used. In addition to making changes directly on the RPI itself, everything can be updated remotely through Bluetooth or Wifi. Interfacing with the RPI is accomplished with a 3" TFT touchscreen display. This simplifies the interaction between the user and the sensor module. This separation of lower and higher level communication allows for the system itself to be divided into two parts: the sensor and the handheld module. This enables the sensor module to be removed from the handheld device and integrated into another system easily. The sensor module by itself can be seen in Figure 3.2 and combined with the handheld module in Figure 3.3.

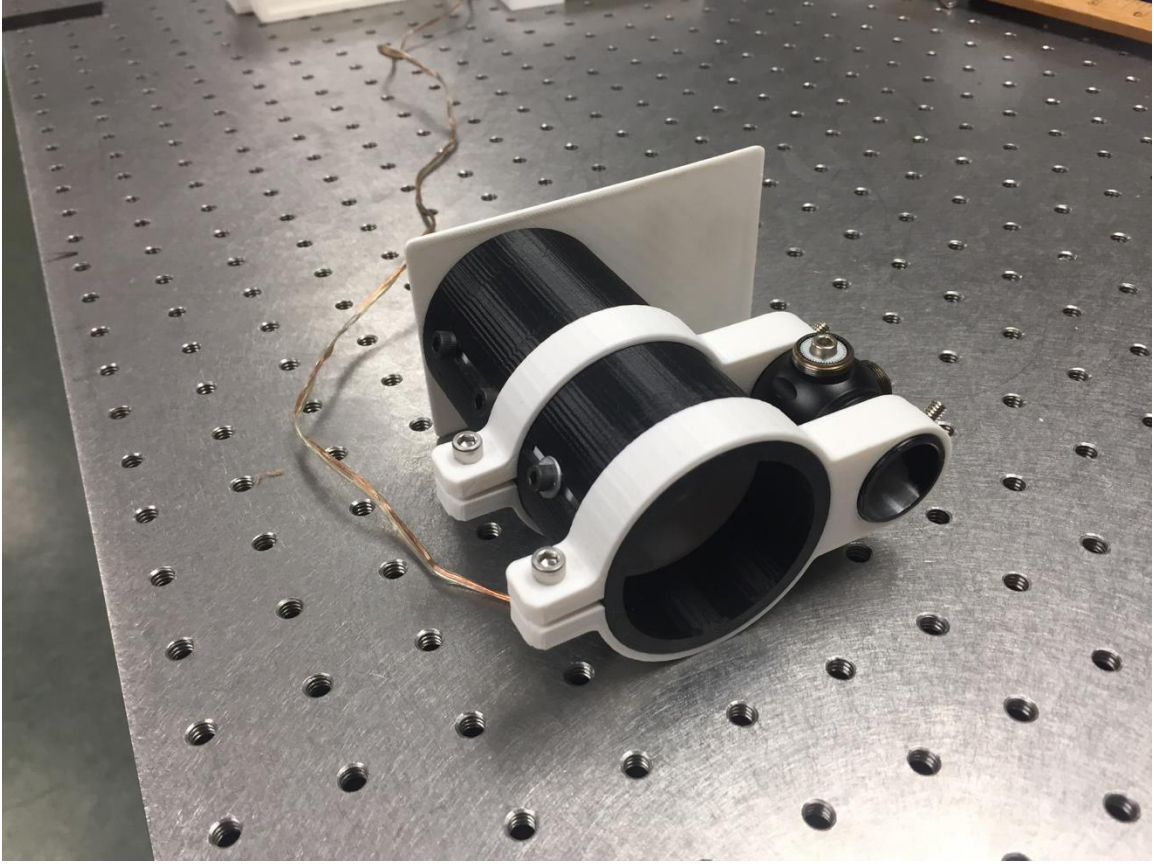


Figure 3.3 The sensor module by itself.

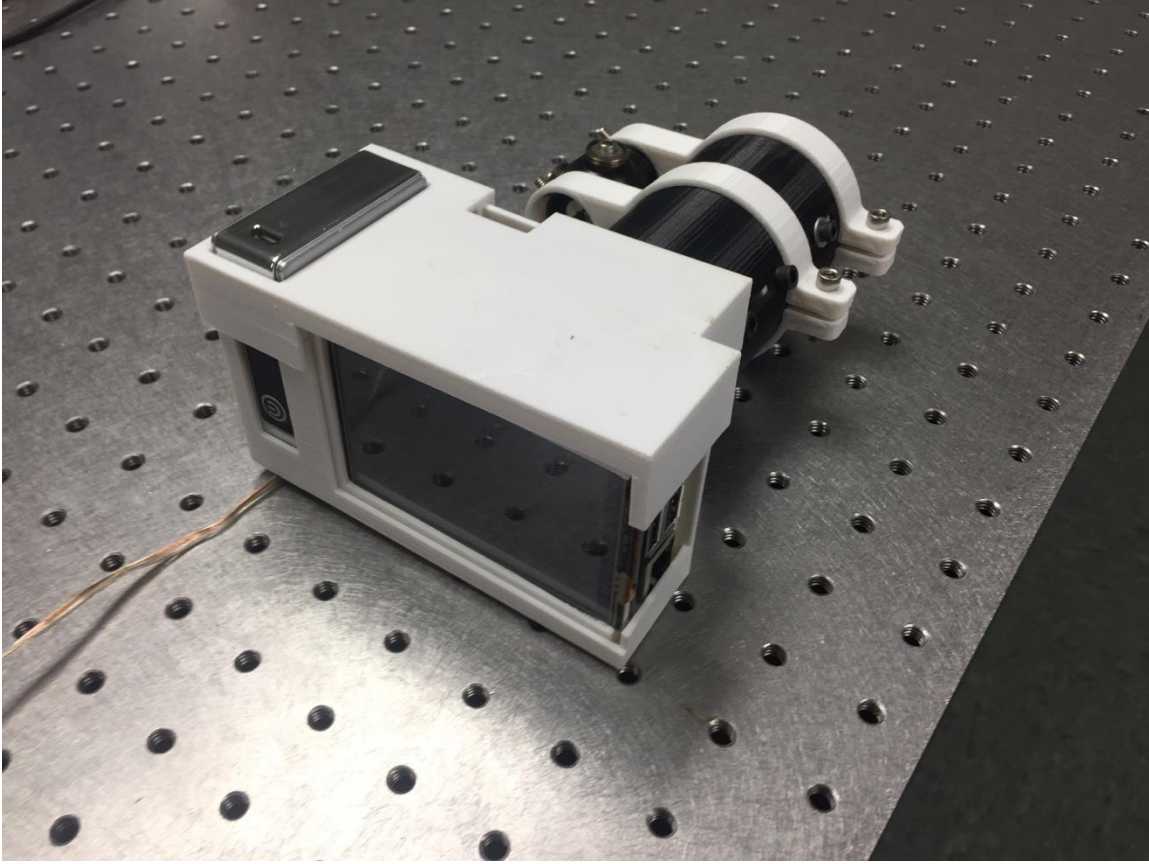


Figure 3.4 The sensor module integrated with the handheld unit.

3.2 Software

All higher-level software in the system was written in Python, an open source programming language. In order to simplify communication between the sensing unit and the RPi, a serial communication protocol was developed. This allows not only the RPi to communicate with the sensing unit, but also any device that can communicate via serial. The protocol gives an easy way for peripherals to control data collection and spectrometer settings. All data visualization and manipulation was done using Python 3 and the dedicated scientific modules SciPy, NumPy, and Matplotlib. This section will

first describe the details of the software that controls the sensor module, followed by a description of the graphical user interface used by the handheld unit.

3.2.1 Spectrometer Control

The code on the Arduino Nano, written for control of the spectrometer and communication with attached devices, is all written in the C programming language. Its main function is to serve as an interpreter from outside commands, most commonly via serial, to the spectrometer. The code controlling the spectrometer directly was adapted from Peter Jansen and the Tricorder project [13]. To communicate, it reads in bytes through serial until it receives its end of line (EOL) character, newline ('\n'). Then, it parses the messages, completes the task, and responds accordingly. Secondary functions include storage of spectrometer data with timestamp to an SD card, control of a status LED, and low level communication via an I/O pin. This last feature allows the triggering and storage of data by merely by the changing of one pin with respect to 5V and ground. When the pin is tied to ground, data collection begins until the pin is tied to 5V, at which time the data is saved.

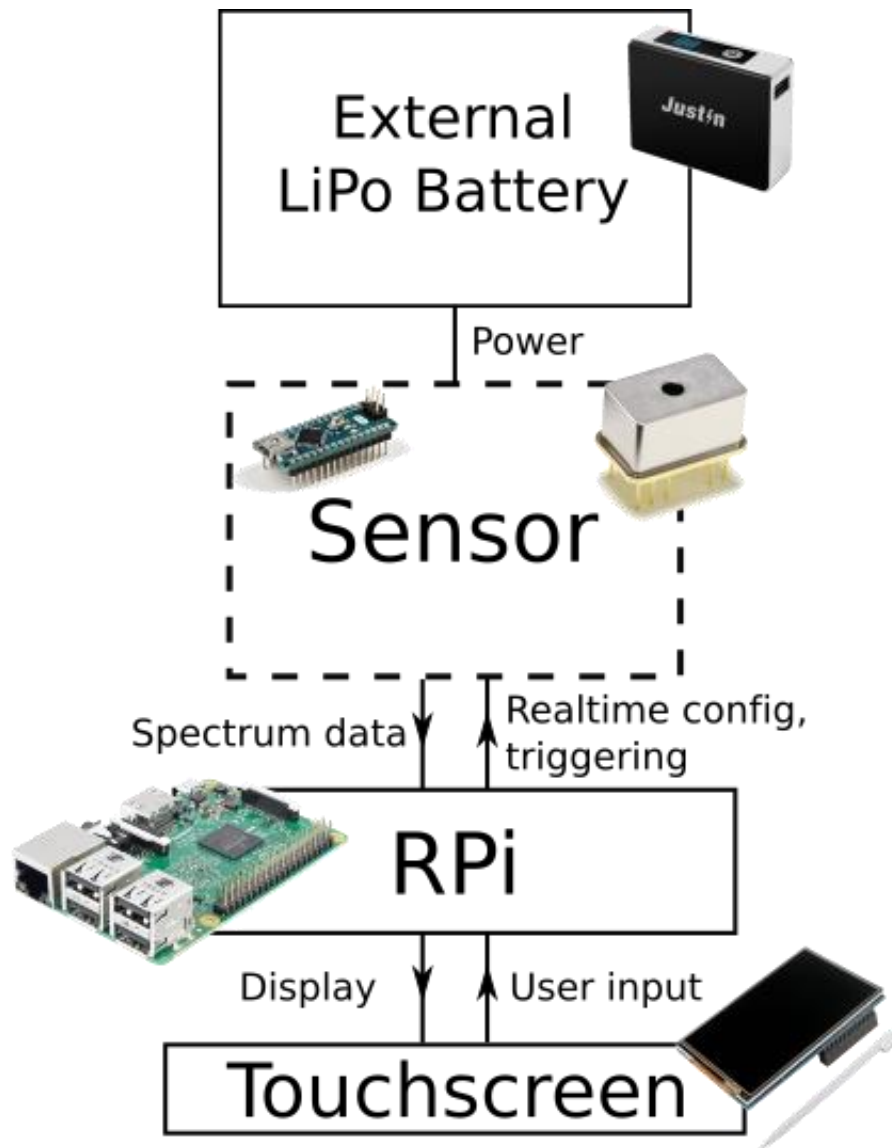


Figure 3.5 Control diagram of the sensor module in the handheld unit

3.2.2 Graphical User Interface (GUI)

The user interface of the handheld device is controlled through the RPi by Python and Qt, a cross platform GUI development framework. This allows the user, through a touch screen, to control the sensor module and to view spectra in real time. Though constantly collecting data, the user can change the integration time, save snapshots of the

data, change the gain, and manipulate the graph's properties such as scale. A screenshot of the graphical user interface (GUI) in action can be seen in Figure 3.1.

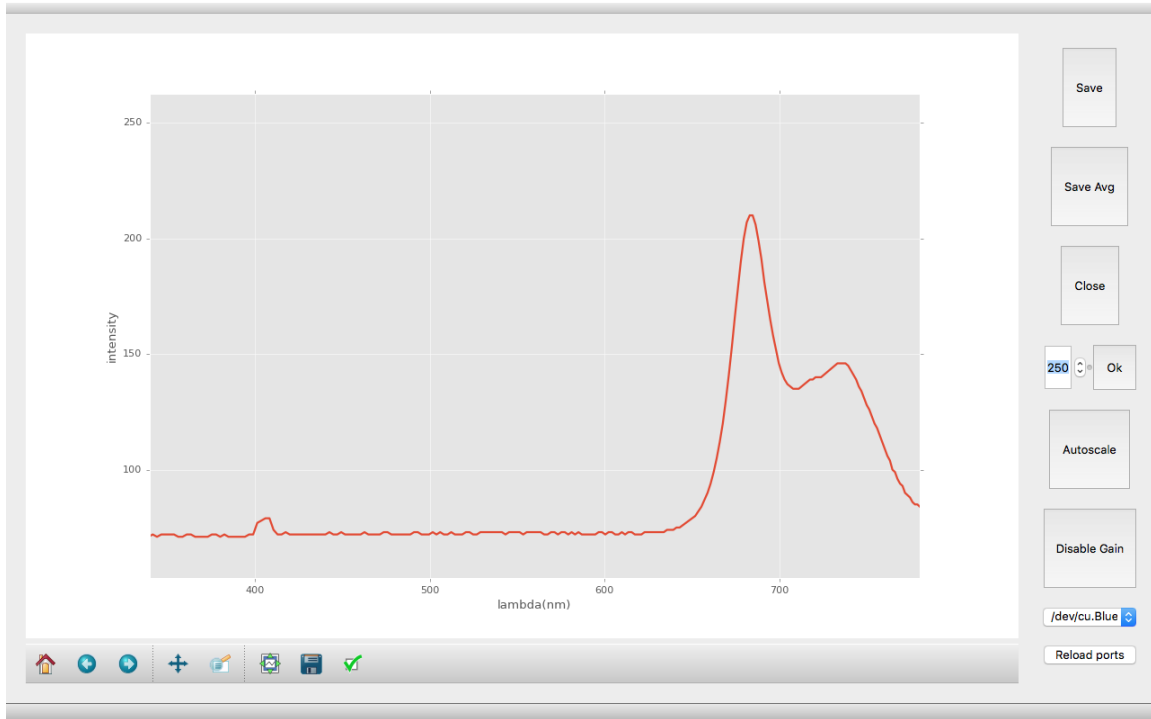


Figure 3.6 Example of GUI

A screenshot example of the GUI on the touchscreen display. Shown is a sample of chlorophyll fluorescence spectrum of a plant leaf.

CHAPTER IV
DATA COLLECTION AND ANALYSIS

4.1 Calibration and Performance Testing

In order to know precise values of measured wavelengths, the spectrometer needs to be calibrated. To accomplish this, a light source with narrow and well-known spectral lines is used: a helium lamp. A quadratic approximation was used to fit the collected calibration data to the reference.

$$\lambda(p) = \lambda(0) + C_1p + C_2p^2 \quad 4.1$$

In the equation, $\lambda(p)$ is the wavelength of pixel p , $\lambda(0)$ is the wavelength at pixel 0 and C_1 and C_2 are the coefficients of the fit. The spectral lines of He and the calibrated spectrometer spectra of He are shown in Figure 4.1.

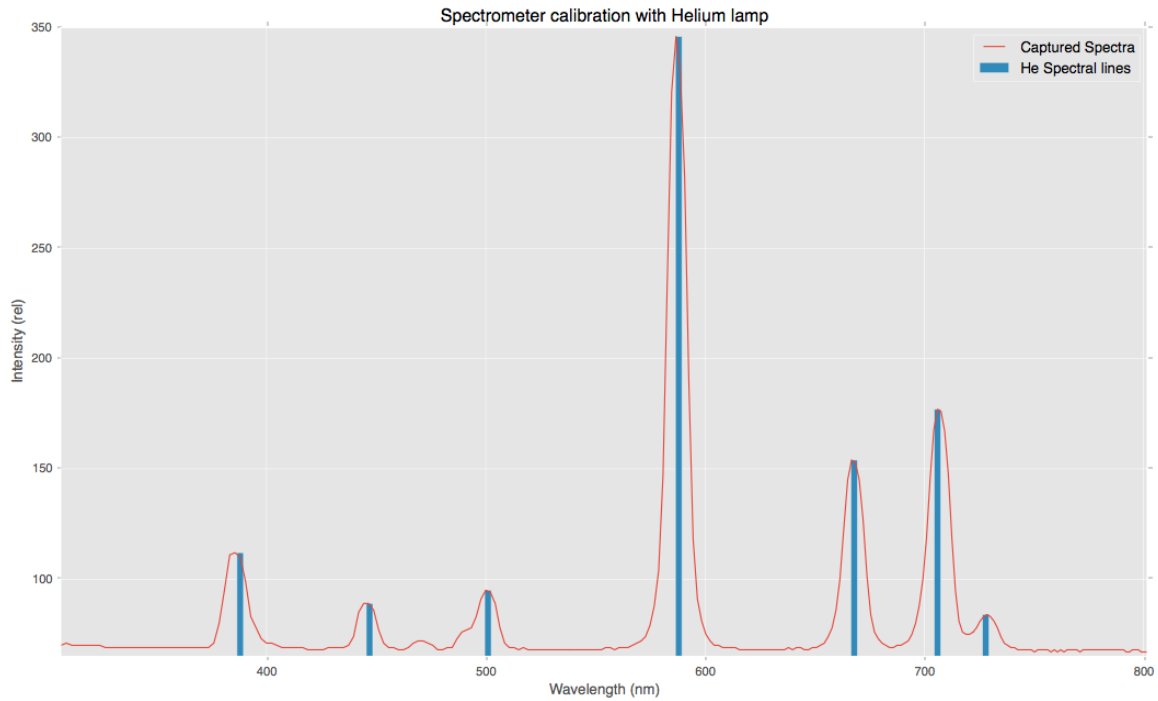


Figure 4.1 Spectrum taken of a helium lamp along with known spectral lines.

Distance testing was also performed using a highly fluorescent target to determine accuracy. For the target, standard multipurpose white paper was chosen. Chemical compounds which fluoresce blue when excited by UV light, are added to paper products as optical brighteners. The blue fluorescence offsets the natural yellowish color of paper to produce an apparently brighter and whiter-looking paper. This fluorescence was measured reliably up to 25 meters.

4.2 Chlorophyll Fluorescence of Vegetation

In vegetation, incident light is absorbed by chlorophyll. The absorbed energy are driving photosynthesis, or be re-emitted as heat or fluorescence. Chlorophyll fluorescence accounts for only a very small percentage of the absorbed light [6], yet it has been used for decades for physiological studies on plants. The main chlorophyll fluorescence peaks

can be found near 690 nm, known as red chlorophyll fluorescence or F690, and 740 nm, known as far-red chlorophyll fluorescence or F740. [5] An example spectrum of chlorophyll fluorescence with a 405 nm excitation source can be seen in Figure 4.1.

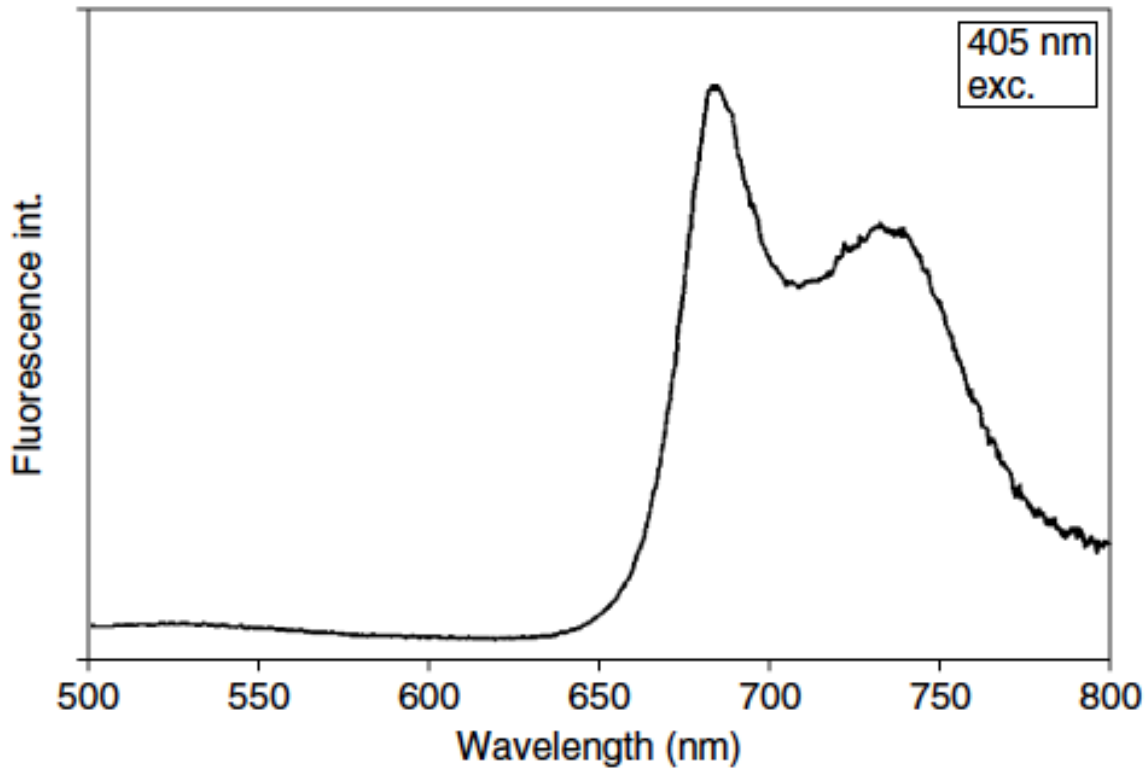


Figure 4.2 Spectra of Spruce at 405nm excitation [1].

While an excellent indicator of photosynthetic efficiency, there are many factors that can influence photosynthesis and subsequently chlorophyll fluorescence [7]. It is therefore a useful measure of a plant's physiological status, though other means are necessary to determine the cause. There have been many studies correlating changes in chlorophyll fluorescence intensity and the ratio of F690 to F740 to stress of various types

[5, 8], fruit ripeness [10, 14], and many other factors. A main focus of this portable LIF module is remote sensing of this red and far-red chlorophyll fluorescence.

To test the performance of this device in regards to chlorophyll fluorescence, several studies were performed. The first of these was to measure chlorophyll fluorescence of leaves on a Water Oak tree. This sample was chosen mainly on the convenience of its proximity and chlorophyll fluorescence signal. Measurements were made both on leaves that appear stressed and ones that appear unstressed. The appearance of stressed was based on a non-uniformity of its color, dark spots dotting its surface, and its decreased size. Shown in Figure 4.3 is a comparison of typical results. A picture of these typical samples is shown in Figure 4.4. A large difference in the total amount of chlorophyll fluorescence between the samples is evident. The ratio F_{690}/F_{740} also had a large difference with 1.50 for the unstressed leaf and 0.67 for the stressed leaf. The distance at which the unstressed fluorescence could be measured was also tested with a reasonable integration time (100 ms) and produced satisfactory results up to 8 m. This distance could be extended using higher integration times. However, holding the device steady on a target becomes difficult at larger distances.

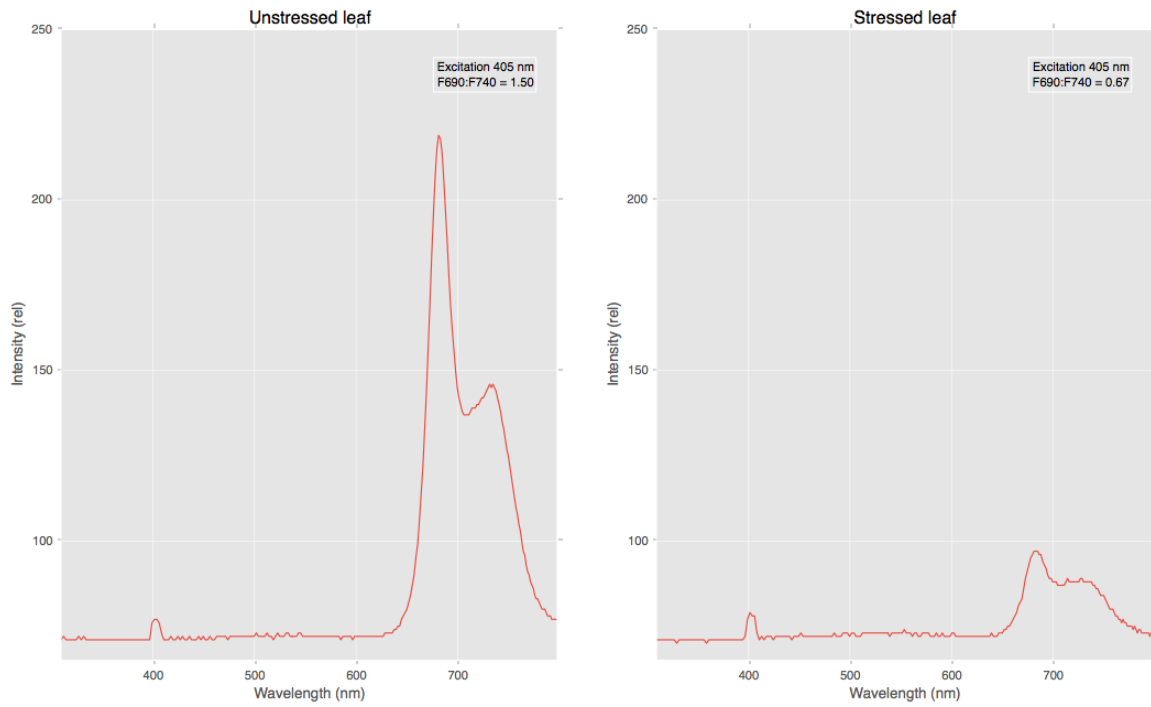


Figure 4.3 Chlorophyll fluorescence spectra of unstressed (left) and stressed (right) water oak leaves.



Figure 4.4 Image of two water oak leaf samples, an unstressed (left) and a stressed (right) leaf.

4.3 Inspection of Fruit Ripeness

The change in the intensity of chlorophyll fluorescence peak F690 has been shown to correspond to the ripeness of various types of fruit, including papaya [14] and apples [10]. As a brief test of the capabilities of this system, chlorophyll fluorescence was measured during the ripening of both granny smith apples and bananas. These two fruits were chosen based on their speed of ripening, visible color changes, and previous studies. Bananas ripen quickly over the course of a few days with a very visible change. Granny Smith apples take longer to ripen and their color is more constant. Over the

course of a week, fluorescence spectra were measured on predetermined spots on apples and bananas using a 405 nm excitation source.

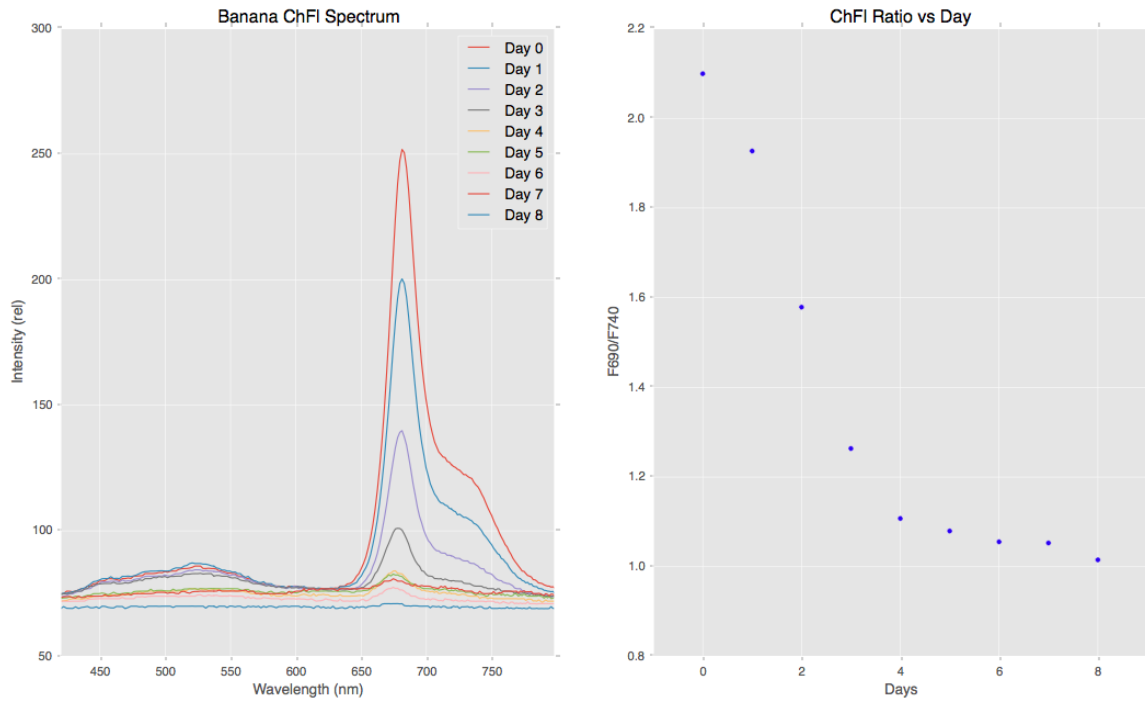


Figure 4.5 Chlorophyll fluorescence of a Banana with the F690/F740 ratio plotted against days.

Figure 4.5 shows both the chlorophyll fluorescence spectra of a banana over the course of several days, along with the ratio of F690 to F740 vs number of days. A clear decrease in the chlorophyll fluorescence is indicative of the banana ripening. This decrease in chlorophyll fluorescence was typical of all samples.

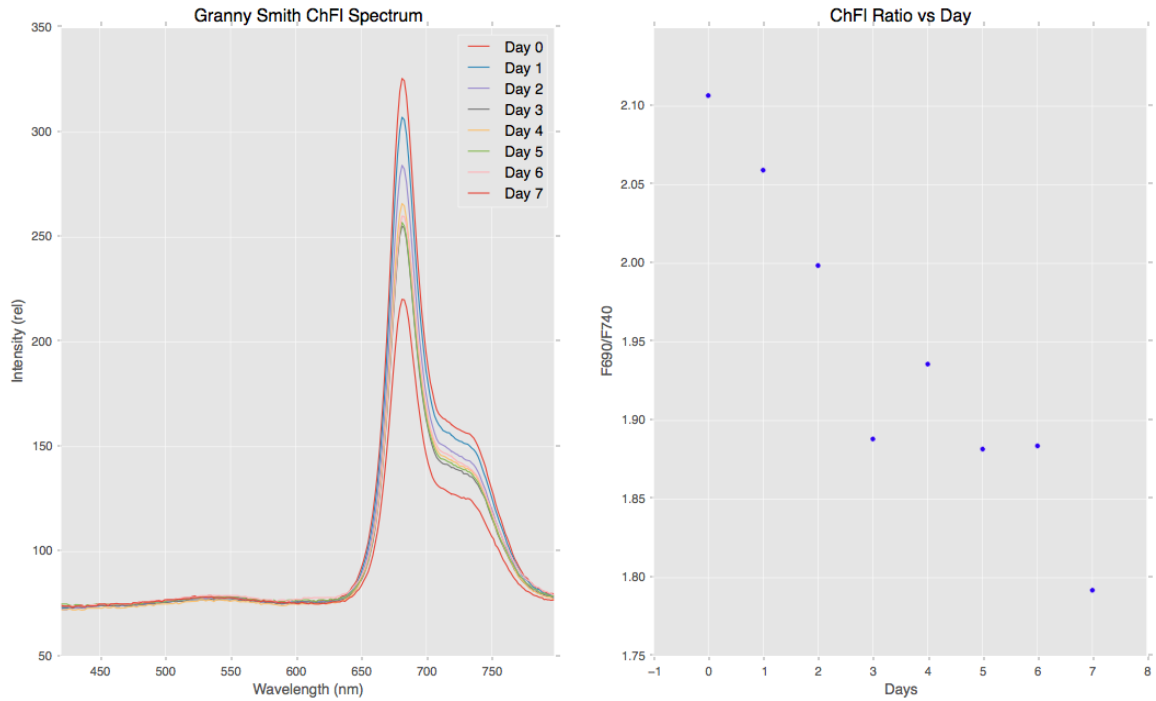


Figure 4.6 Chlorophyll fluorescence of a Granny smith apple with the F690/F740 ratio plotted against days.

Figure 4.6 shows the same graph for a typical granny smith apple sample. There is a downward trend in the F690/F740 ratio, however not as dramatic as bananas. This method of non-invasive ripening detection could be used for rapid assessment of produce in stores or in homes.

4.4 Aflatoxin Detection

Another useful application of LIF spectroscopy in agriculture is the identification and quantification of diseases present in plants [11, 9]. Among diseases affecting crops, aflatoxin and various similar fungal toxins are widely studied diseases. Aflatoxin is a carcinogenic toxin produced by the *Aspergillus Flavus* fungi which can affect corn, wheat, rice and peanuts among others. The fungal infection *A. Flavus* has been shown to

produce fluorescence from UV excitation with a peak around 450 nm [11]. This fluorescence signal is referred to as blue greenish-yellow (BGY). Though not a direct measure of the presence of aflatoxin in a sample showing BGY fluorescence, it is an indicator that aflatoxin could be present. Samples of corn kernels containing aflatoxin were obtained for a test of the aflatoxin detection ability of this portable LIF sensor. Both kernels inoculated with aflatoxin and those without inoculation were sampled several times using the sensor module. The results are shown in Figure 4.2.

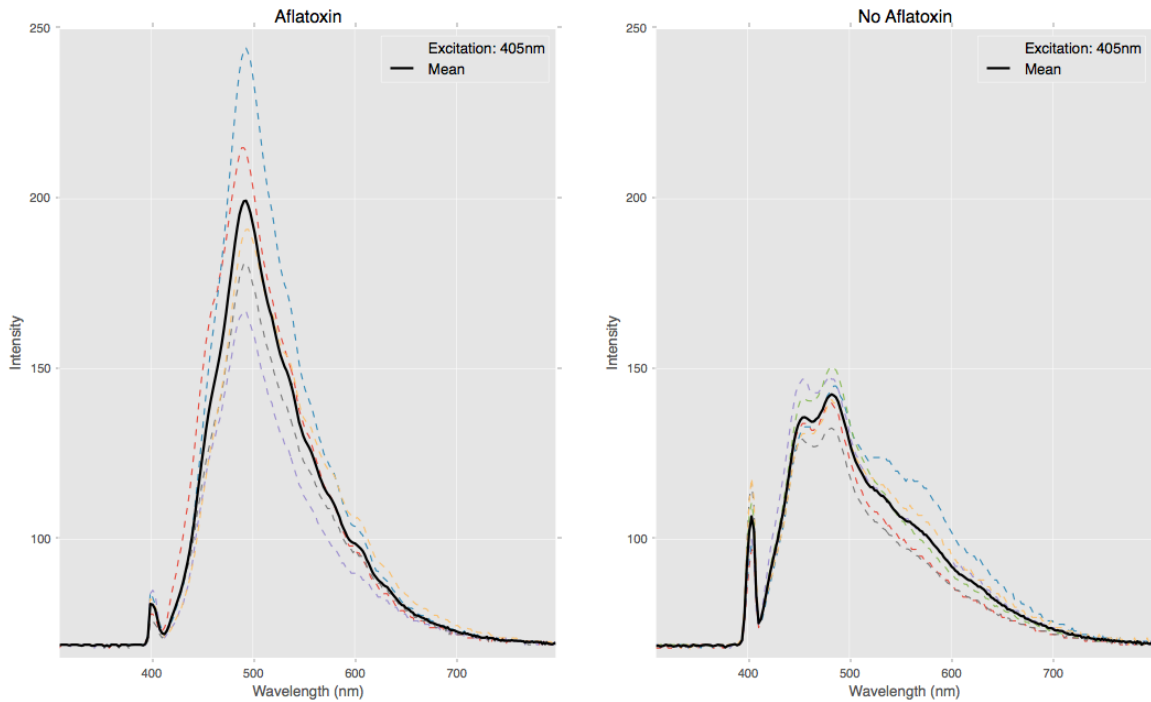


Figure 4.7 Fluorescence spectra collected from kernels with and without aflatoxin present

The bold black line is the average of all samples, while the faint dotted lines are the samples themselves.

As seen in Figure 4.2, there is a distinct difference in the amount of fluorescence from infected versus non infected corn kernels. While not a rigorous test, it demonstrates

the potential ability for this portable device to quickly identify potentially infected samples of corn. These results are consistent with other work showing an increase in BGY fluorescence in the presence of aflatoxin. [12]

CHAPTER V

CONCLUSION AND FUTURE WORK

5.1 Ongoing Work

Further research is already underway to use the sensing module as a part of an unmanned aerial vehicle (UAV). As part of its original design, the sensor module is intended to integrate with other devices, especially with a UAV. A UAV has already been built for the purpose of carrying and testing remote sensing equipment in flight. The optics system chosen for the final design of the sensor module was chosen in part so it would be smaller and lighter weight. This makes mounting to the UAV easier, and a lighter weight translates to more efficiency. The UAV is built on open source hardware, the APM2.6 flight controller, and open source software, ArduCopter. It has an onboard sensor suite, including magnetometers, accelerometers, and gyroscopes for linear and angular position, rotation and acceleration. A combination of an ultrasonic rangefinder and a barometer determine altitude, and a GPS with magnetometer determine global position and heading. All of this information is transmitted and logged via a radio telemetry link to a ground control station. This gives the UAV the ability to autonomously fly preplanned missions. The sensor module mounts to the UAV on a servo-driven gimbal mount which aims the device directly downward regardless of the UAV's rotation. The Arduino controller on the sensor module has one-way communication with the UAV via the I/O pin. This pin triggers the sensor module to start

collecting data constantly, and store it on an onboard SD card along with a timestamp. After the mission, the data collected by the sensor module and the data logged by the UAV can be coupled and reconstructed into an image. A diagram of this control scheme is shown in Figure 5.2

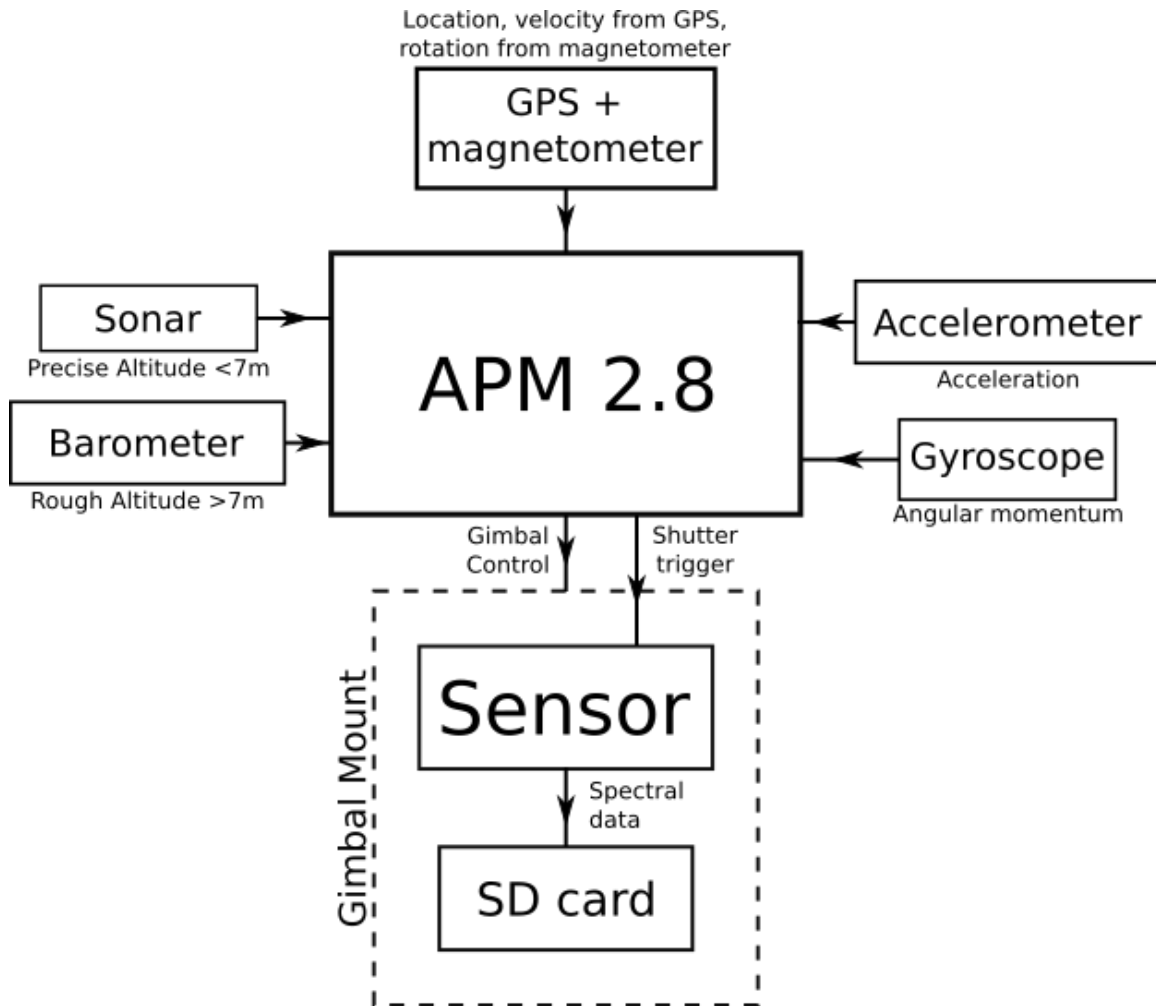


Figure 5.1 A Control diagram for the sensor module and UAV electronics

The goal of this work will be to reconstruct an image of the F690:F740 ratio of a field of crops to map changes in stress among crops being grown. In addition to aerial

measurements, the ability for the sensor module to be easily switched into another device will allow for follow up measurements in the field. This could help diagnose disease or infestation detection or undesirable soil content or water flow. A secondary goal is to have the UAV and sensor module both be as inexpensive as possible while maintaining effectiveness. The total projected cost of the currently designed system is less than \$1000.

5.2 Conclusion

This work describes the design and construction of a laser induced fluorescence sensor module, along with an accompanying handheld device for display and manipulating its output. The sensor was made to be lightweight, portable, cost-effective, and modular, and thus the objective for the device is complete. As a test of the LIF sensor's performance, the results from several different experiments are shown. The sensor module is shown to be able to monitor ripeness in fruit, detect stress in tree leaves, and indicate the presence of a carcinogenic fungal toxin in corn. The integration of the sensor module into another platform, an unmanned aerial vehicle, is also discussed. With this continuing work, this portable laser induced fluorescence sensor will be taking practical and useful chlorophyll fluorescence data in a field setting in the very near future.

5.3 Future Work

There are several optimizations and extensions to the sensor module that could be completed. A more robust, collinear optics system could be designed, though the risk of difficulty in aligning the optics and an increase in cost are still present. Since beginning

this work, Hamamatsu Photonics has released a newer version of the C12666MA spectrometer, the C12880MA. This version boasts a higher sensitivity and slightly larger wavelength detection range. This could be easily implemented into the current design. The physical design of the casing, while functional, could be improved to be more aesthetically pleasing. Finally, more features could easily be built into the GUI of the handheld system, such as visualizing and manipulating data already collected.

There are many potential systems into which the sensor module could be integrated. Bluetooth could be added to the sensor module to allow for remote communication with smartphones, tablets or computers. The sensor module has already been mounted on a UAV for in flight measurements, and the device could also be mounted on a boat or on a tractor directly in the field. As for the detection of aflatoxin in corn, the sensor module could potentially be used in a device that screens harvested corn as it is moved on a conveyor system. Lastly, an alternative optics set up using a fiber optic cable for light collection could be used for point measurement of fluorescence.

REFERENCES

1. S. Svanberg, "Fluorescence spectroscopy and imaging of lidar targets," *Laser Remote Sensing*, T. Fujili and T. Fukuchi, eds. pp. 433-467 (CRC Press, 2005)
2. S. Andersson-Engels, C. af Klinteberg, K. Svanberg and S. Svanberg, "In vivo fluorescence imaging for tissue diagnostics," *Phys. Med. Bio.* **42**(5), pp. 815-824 (1997).
3. P. Chen, D. Pan, Z. Mao, "Development of a portable laser-induced fluorescence system used for in situ measurements of dissolved organic matter," *Optics and Laser Tech.* **64**, pp. 213-219 (2014).
4. J. McMurtrey III, E. Chappelle, M. Kim, L. Corp and C. Daughtry, "Blue-green Fluorescence and Visible-infrared Reflectance of Corn (*Zea mays* L.) Grain for *in situ* Field Detection of Nitrogen Supply," *J. Plant Physiol.* **148**, pp. 509-514 (1996).
5. H. Lichtenthaler, and J. Miede, "Fluorescence imaging as a diagnostic tool for plant stress," *Trends in Plant Science*, **2**(8), pp. 316-320 (Elsevier Science Ltd, 1997).
6. K. Maxwell, and G. Johnson, "Chlorophyll fluorescence – a practical guide," *Journal of Exp. Bot.* **51**(345), pp. 659-668 (2000).
7. Z. Cerovic, G. Samson, F. Morales, N. Tremblay, and I. Moya, "Ultraviolet-induced fluorescence for plant monitoring: present state and prospects," *Agronomie*, **19**(7) pp. 543-578 (EDP Sciences, 1999).
8. J. Belasque, Jr, M. C. G. Gasparoto, and L. G. Marcassa, "Detection of mechanical and disease stresses in citrus plants by fluorescence spectroscopy," *Applied Optics*, **47**(11), pp. 1922-1926 (2008).
9. E. Lins, J. Belasque, Jr, L. Marcassa, "Detection of citrus canker in citrus plants using laser induced fluorescence spectroscopy," *Precision Agric.* **10**, pp. 319-330 (2009).
10. A. Das, A. Wahi, I. Kothari, and R. Raskar, "Ultra-portable, wireless smartphone spectrometer for rapid, non-destructive testing of fruit ripeness," *Nature Scientific Reports*, **6**, p 32504 (2016).

11. M. Rodriguez, G. Sanchez, M. Sobrero, A. Schenone, N. Marsili, "Determination of mycotoxins (aflatoxins and ochratoxin A) using fluorescence emission-excitation matrices and multivariate calibration," *Microchemical Journal*, **110**, pp. 480-484 (2013).
12. H. Yao, Z. Hruska, R. Kincaid, R. Brown, T. Cleveland, and D. Bhatnagar, "Correlation and classification of single kernel fluorescence hyperspectral data with aflatoxin concentration in corn kernels inoculated with *Aspergillus flavus* spores," *Food Additives & Contaminants: Part A*, **27**(5), pp. 701-709 (2010).
13. P. Jansen, <https://www.tricorderproject.org>.
14. I. Bron, R. Riberio, M. Azzolini, A. Jacomino, E. Machado, "Chlorophyll fluorescence as a tool to evaluate the ripening of 'Golden' papaya fruit," *Postharvest Biology and Technology*, **33**, pp. 163-173 (2004).

APPENDIX A
MATERIALS

A.1 Cost Breakdown

Table A.1 An itemized listing with costs for all parts used

Sensor Unit	
Item	Cost
Hamamatsu C12666MA Spectrometer	\$308
Arduino Nano	\$4
SD card read for Arduino	\$2
405 nm Laser	\$15
2" NBK-7 60mm Lens	\$36
420nm LP Colored Glass Filter	\$25.50
3D Printed Parts for housing (estimate)	\$2
Subtotal	\$392
Handheld Unit	
Item	Cost
5 Ah 2A 5v USB Battery pack	\$16.99
Raspberry Pi 3 Model B	\$38
32 GB MicroSD card	\$15.85
3.5" Resistive TFT Touchscreen	\$19.99
3D Printed Parts for housing (estimate)	\$2
Subtotal	\$92.83
Total	\$484.83